Int. J. Dev. Biol. 54: 815-825 (2010)
doi: 10.1387/ijdb.082841lp

THE INTERNATIONAL JOURNAL OF DEVELOPMENTAL BIOLOGY
www.intjdevbiol.com

A novel role for *Glucocorticoid-Induced TNF Receptor Ligand (Gitrl)* in early embryonic zebrafish development

LYNN D. POULTON[1,a,c], KATHLEEN F. NOLAN*[,1,a], CORINA ANASTASAKI[2], HERMAN WALDMANN[1,b] and E. ELIZABETH PATTON[2,b]

[1]*Sir William Dunn School of Pathology, University of Oxford, Oxford, and* [2]*Institute of Genetics and Molecular Medicine, MRC Human Genetics Unit and The University of Edinburgh, Edinburgh, UK*

ABSTRACT Tumour necrosis factor ligand and receptor superfamily (TNFSF and TNFRSF) members have diverse and well-studied functions in the immune system. Additional, non-immunological roles, such as in the morphogenesis of bone, tooth, hair and skin have also been described for some members. GITRL and its receptor GITR are well-described as co-regulators of the mammalian immune response. Here, we describe the identification and cloning of their zebrafish homologues and demonstrate a novel role for the ligand, but not the receptor, in early vertebrate development. The assignment of zebrafish Gitrl and Gitr was supported by homology and phylogenetic analysis. The ligand exhibited an oscillating pattern of mRNA expression during the first 36 hours post fertilization, during which time *gitr* mRNA was not detected, and morpholino oligonucleotide-mediated knock-down of *gitrl*, but not of *gitr*, resulted in disruption of early embryogenesis, most clearly revealed during gastrulation, which corresponded to the earliest peak in *gitrl* mRNA expression (5.25-10 hpf). We found Stat3 signalling to be altered in the *gitrl*-morphants, suggesting that one possible role for Gitrl during embryogenesis may be modulation of Jak/Stat signalling.

KEY WORDS: *GITRL, GITR, development, zebrafish, Stat3*

Introduction

The TNF and TNFR superfamilies are receptor-ligand signalling molecules that regulate a variety of pathways, but have primarily been associated with the maintenance and regulation of the immune system. One of these, the glucocorticoid-induced TNF receptor (GITR), in addition to being expressed on activated effector T cells, was also highlighted in a screen for genes expressed by regulatory T cells (Zelenika *et al.*, 2002). Regulatory T cells engage in the suppression of activated effector T cells, including self-reactive T cells, thereby controlling the immune response and helping to prevent autoimmunity. The ligand for GITR, GITRL, is constitutively expressed on antigen presenting cells. Its expression is transiently increased in response to inflammatory stimuli, and engagement of GITR by GITRL leads to both dampening of the suppressive effects of regulatory T cells, and to co-activation of effector T cells (Tone *et al.*, 2003). The net effective outcome is strong activation of the immune response, and indeed, antibody-mediated stimulation of GITR can induce autoimmunity (Shimizu *et al.*, 2002). The potential to modulate immune regulation through GITRL-GITR signalling has made this pathway an interesting candidate for study in cancer immunotherapy and in models of persistent infection.

In mice, targeted disruption of the GITR gene results in T cell hypersensitivity to CD3 activation, leading to hyperproliferation and heightened sensitivity to activation-induced cell death (Ronchetti *et al.*, 2002), as well as altered responses to *Candida*

Abbreviations used in this paper: dpf, days post-fertilization; EDA, ectodysplasin; hpf, hours post fertilization; GITR, glucocorticoid-induced TNF receptor; GITRL, glucocorticoid-induced TNF receptor ligand; MO, morpholino oligonucleotide; TNFSF, tumour necrosis factor superfamily; TNFRSF tumour necrosis factor receptor superfamily.

***Address correspondence to:** Dr. Kathleen F Nolan. Sir William Dunn School of Pathology, University of Oxford, South Parks Road, Oxford, OX1 3RE, UK. Fax: +44 (0)1865-275501. e-mail: kathleen.nolan@path.ox.ac.uk

Notes: [a]L.D.P and K.F.N contributed equally to this work. [b]H.W. and E.E.P. contributed equally to this work. [c]Present Address: Arana Therapeutics, Epping Rd, Macquarie Park NSW 2113 Australia

Accepted: 2 June 2009. *Final author-corrected PDF published online:* 3 July 2009.

ISSN: Online 1696-3547, Print 0214-6282
© 2009 UBC Press
Printed in Spain

albicans (Agostini *et al.*, 2005) and in experimentally induced acute lung inflammation (Cuzzocrea *et al.*, 2006). With a specific interest in the role of GITRL in these phenomena, and anticipating an immune phenotype similar to that seen in the *Gitr* knockout, we generated a mouse knockout of the GITRL gene and were surprised by a strain-dependent embryonic lethal phenotype that suggested an essential role for GITRL in development (manuscript in preparation). To gain specific insight into the developmental requirements for GITRL we turned to the zebrafish system, now widely used as a complementary vertebrate model for studies in both immunology and development.

A role for the TNF/TNFR families in the development of non-lymphoid tissues has precedents. Although initially highlighted for its role in the immune system, RANKL has been shown to be essential for osteoclast differentiation and bone remodelling in mice, as well as lymph-node organogenesis and the early differentiation of thymocytes and B cell precursors (Kong *et al.*, 1999), while in humans mutations in *RANKL* underlie autosomal recessive osteoclast-poor osteopetrosis (Frattini *et al.*, 2007). Ectodysplasin (EDA) is the only TNFSF member to date whose function remains exclusively non-immune. Mutations in EDA in mice (*Tabby*) affect development of the skin, hair and teeth (Ferguson *et al.*, 1997), and similarly in humans are causative of X-linked anhidrotic ectodermal dysplasia, a disorder characterised by sparse hair, absence of sweat glands and abnormal or missing teeth (Kere *et al.*, 1996).

Here we describe the identification of genes encoding homologues of mammalian GITRL and GITR in zebrafish. We have cloned the corresponding ligand and receptor transcripts and demonstrate, by differential gene expression and morpholino oligonucleotide (MO)-mediated gene knockdown, a critical role for the ligand in early embryonic development. This role is

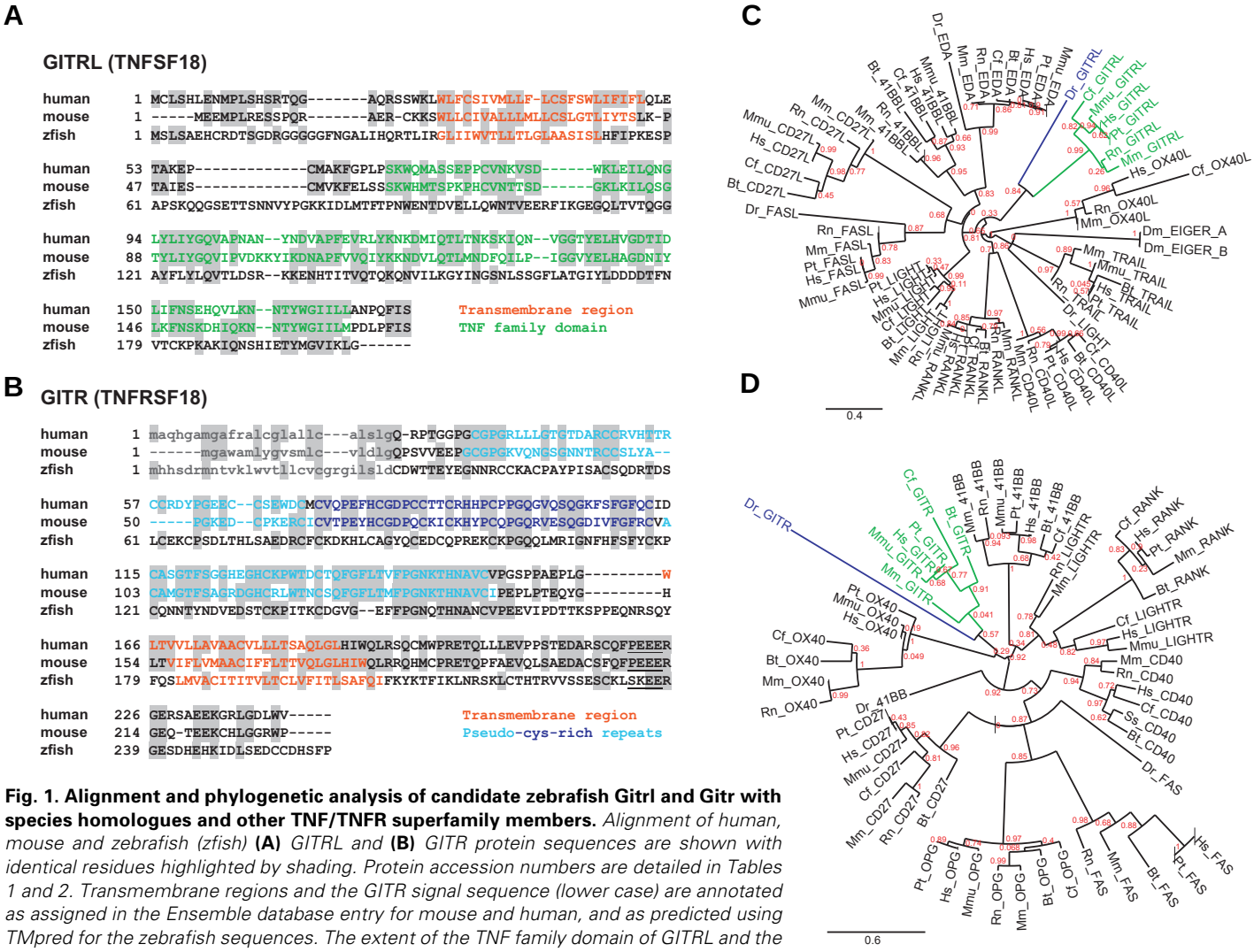

Fig. 1. Alignment and phylogenetic analysis of candidate zebrafish Gitrl and Gitr with species homologues and other TNF/TNFR superfamily members. *Alignment of human, mouse and zebrafish (zfish)* **(A)** *GITRL and* **(B)** *GITR protein sequences are shown with identical residues highlighted by shading. Protein accession numbers are detailed in Tables 1 and 2. Transmembrane regions and the GITR signal sequence (lower case) are annotated as assigned in the Ensemble database entry for mouse and human, and as predicted using TMpred for the zebrafish sequences. The extent of the TNF family domain of GITRL and the three pseudo-cysteine rich domains of GITR are marked as their respective Ensemble and Uniprot database entries. A TRAF-2 binding consensus (P/S/A/T)x(Q/E)E conserved in the cytoplasmic tail of GITR is underlined (Ye* et al.*, 1999). Phylograms generated using selected* **(C)** *TNF and* **(D)** *TNFR superfamily members confirmed that the cloned zebrafish sequences cluster with mammalian homologues of GITRL and GITR respectively. The analyses were performed using nucleotide coding sequences extracted from database entries detailed in Tables 1 and 2. Branch support based on an approximation of the standard likelihood ratio test is indicated (Dereeper* et al.*, 2008). Synteny information to support the assignment of species homologues was established, except for Dr_GITR, Dr_GITRL, Dr_EDA, Dr_LIGHT and Dr_FasL.*

independent of the cloned Gitr sequence, but is associated with changes in Stat3 phosphorylation.

Results

Identification and cloning of homologues of GITRL and GITR in zebrafish

Exons of zebrafish *gitrl* and *gitr* were provisionally identified by homology using BLAST, and their corresponding transcripts (Zebrafish *Gitrl* and *Gitr* Genbank accession numbers, EU099310 and EU099311) amplified and cloned from adult zebrafish kidney. The translated sequences were found to share 17-22% amino acid identity with their mouse and human counterparts (Fig. 1 A,B), a level consistent with those previously reported for a number of other fish TNFSF members (Glenney and Wiens, 2007). The human and mouse GITRL and GITR proteins share only 51-58% identity. The candidate *gitrl* cDNA was also subsequently cloned from whole zebrafish embryos to confirm that the embryonic sequence was identical to the adult.

To further establish the assignment of the newly cloned zebrafish TNF and TNF receptor superfamily members, phylogenetic analyses were performed using well-defined species homologues of a selection of ligand and receptor superfamily members, mainly selected on the basis of close homology or by virtue of their genetic locus. TNF superfamily members with well-described roles in development, RANKL and EDA, and the earliest known TNF family member, EIGER (Moreno *et al.*, 2002), were also included. Both the zebrafish ligand and receptor nucleotide coding sequences grouped appropriately with mammalian species homologues of GITRL and GITR respectively (Fig. 1 C,D)

Gitrl, *but not* gitr, *is expressed during the first two days of embryogenesis*

Using real-time PCR analysis, *gitrl* and *gitr* were both found to be transcribed in the lymphoid tissues of adult zebrafish including the kidney marrow (Fig. 2A). The ligand was additionally detected in non-lymphoid tissues of the ovary and brain (Fig. 2A). During the first 36 hours of embryonic development, the ligand exhibited a multiphasic expression pattern (Fig. 2B). An early peak (0-2 hpf), presumably representing maternal mRNA prior to the start of zygotic transcription, dropped away rapidly. Expression reappeared during gastrulation (5.25-10 hpf), rising to a peak corresponding to the start of segmentation (10.5 hpf). From here, expression dipped as segmentation proceeded, rising again to peak during late segmentation (approx. 18 hpf) with another, lower, peak at 24 hpf (early pharyngula). This oscillating pattern of expression suggests that Gitrl may act at multiple time points during the first 36 hours of development. In contrast, *gitr* expres-

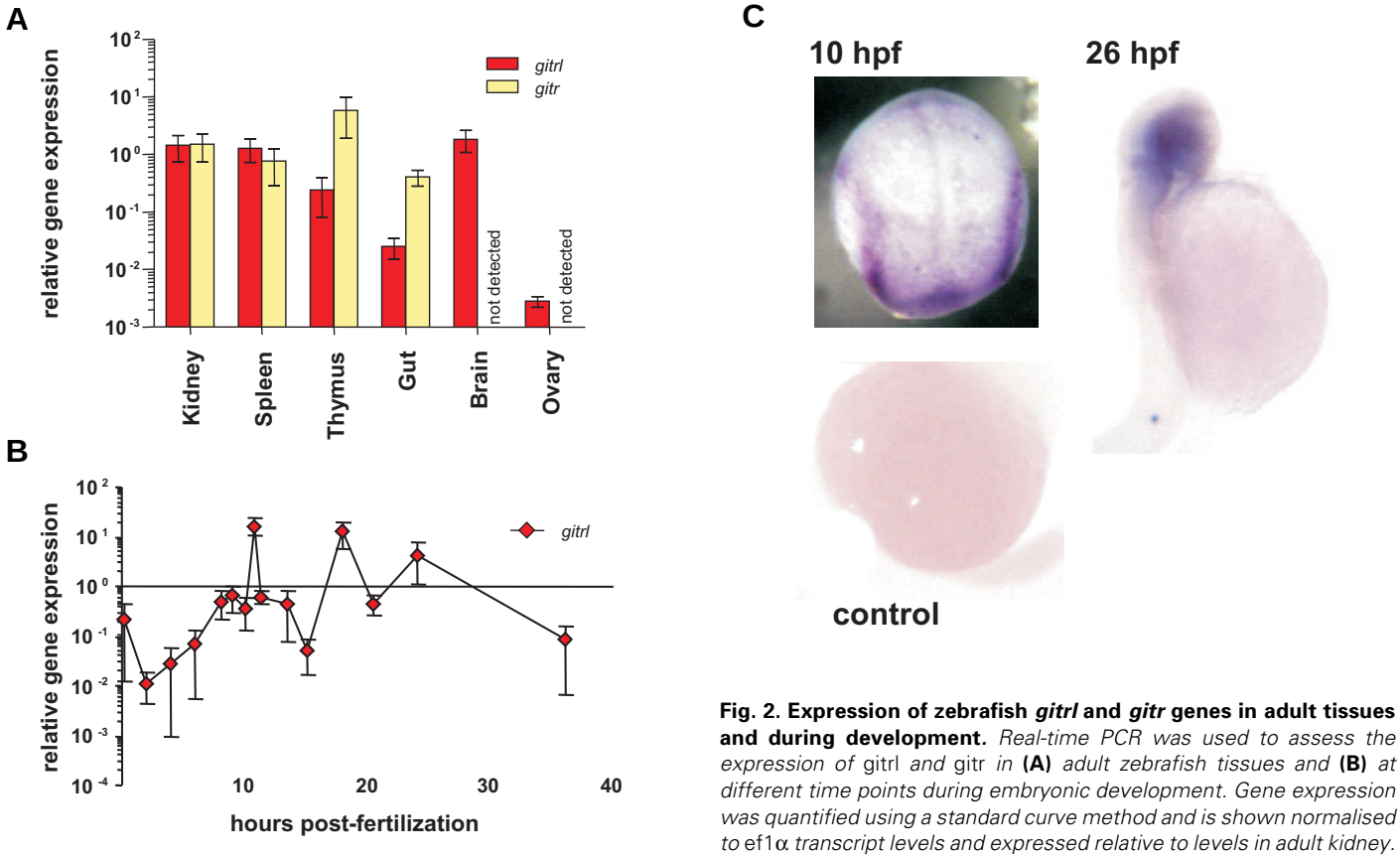

Fig. 2. Expression of zebrafish *gitrl* and *gitr* genes in adult tissues and during development. *Real-time PCR was used to assess the expression of* gitrl *and* gitr *in* **(A)** *adult zebrafish tissues and* **(B)** *at different time points during embryonic development. Gene expression was quantified using a standard curve method and is shown normalised to* ef1α *transcript levels and expressed relative to levels in adult kidney. Values are shown as mean ± SD of technical triplicates for an individual experiment representative of three biological replicates. In adult tissues* gitr *mRNA was not detected in brain or ovary. In embryos, only* gitrl *is shown as no* gitr *mRNA was detected during this period.* **(C)** *Localisation of* gitrl *transcripts at different time-points within developing embryos was investigated by* in situ *hybridization using a DIG-labelled antisense RNA probe. Distinct bands along the paraxial mesoderm can be seen at 10 hpf, with localization of expression to the head region by 26 hpf. A control embryo processed at 16 hpf in the absence of probe is shown to indicate the level of background staining and any yolk trapping.*

sion was undetectable during this period.

To assess localization patterns corresponding to the temporal variations described, wild-type embryos were probed for the presence of *gitrl* mRNA at various early developmental time-points using whole-mount *in situ* hybridization. Transcription was ubiquitous during the first 8 hpf, with some concentration of expression to the germ ring during early gastrulation (data not shown). In late gastrulation and early segmentation, distinct bands of patterning were evident along the paraxial mesoderm (Fig. 2C, 10 hpf). By late segmentation, low expression of *gitrl* was detectable in the anterior of the embryo, which by the mid-pharyngula period had localised to the head region (Fig. 2C, 26 hpf).

Expression of gitrl*, but not* gitr*, is required during early development*

The patterning of *gitrl* expression (Fig. 2B, C) suggested to us that it might have specific functions during embryogenesis. To explore this possibility, we used MOs to knock down *gitrl* expression and embryos were monitored for the emergence of morphological abnormalities. Although the presence of *gitr* mRNA had not been detected in the first two days post-fertilization, the possibility of very low, but functionally relevant levels of expression prompted us to test *gitr* MOs as well. One translation-block (zGL1, zGR1) and one splice-block (zGL2, zGR2) MO were tested for each gene. Both ligand MOs gave a similar dose-dependent mutant embryonic phenotype (Fig. 3A), which was not observed with *gitr*

TABLE 1

TNFSF MEMBERS USED FOR PHYLOGENETIC ANALYSIS

Label in tree (Fig.1)	Protein	Species	Transcript accession #	Protein accession #
Dm_EIGER_A	EIGER, isoform A	*Drosophila melanogaster*	NM_165735	NP_724878
Dm_EIGER_B	EIGER, isoform B	*Drosophila melanogaster*	NM_206069	NP_995791
Bt_EDA	Ectodysplasin-A	*Bos taurus*	NM_001081743	NP_001075212
Cf_EDA	Ectodysplasin-A	*Canis lupus familiaris*	NM_001014770	NP_001014770
Hs_EDA	Ectodysplasin-A	*Homo sapiens*	NM_001399	NP_001390
Mm_EDA	Ectodysplasin-A	*Mus musculus*	NM_010099	NP_034229
Mmu_EDA	Ectodysplasin-A	*Macaca mulatta*	XM_001082424	XP_001082424
Pt_EDA	Ectodysplasin-A	*Pan troglodytes*	XM_529025	XP_529025
Rn_EDA	Ectodysplasin-A	*Rattus norvegicus*	XM_228582	XP_228582
Cf_OX40L	TNFSF4	*Canis lupus familiaris*	XM_547459	XP_547459
Hs_OX40L	TNFSF4	*Homo sapiens*	NM_003326	NP_003317
Mm_OX40L	TNFSF4	*Mus musculus*	NM_009452	NP_033478
Rn_OX40L	TNFSF4	*Rattus norvegicus*	NM_053552	NP_446004
Bt_CD40L	TNFSF5	*Bos taurus*	NM_174624	P51749
Hs_CD40L	TNFSF5	*Homo sapiens*	NM_000074	NP_000065
Mm_CD40L	TNFSF5	*Mus musculus*	NM_011616	NP_035746
Rn_CD40L	TNFSF5	*Rattus norvegicus*	NM_053353	NP_445805
Dr_FASL	TNFSF6	*Danio rerio*	NM_001042701	NP_001036166
Hs_FASL	TNFSF6	*Homo sapiens*	NM_000639	NP_000630
Mm_FASL	TNFSF6	*Mus musculus*	NM_010177	NP_034307
Mmu_FASL	TNFSF6	*Macaca mulatta*	NM_001032838	NP_001028010
Pt_FASL	TNFSF6	*Pan troglodytes*	XM_524967	XP_524967
Rn_FASL	TNFSF6	*Rattus norvegicus*	NM_012908	NP_037040
Bt_CD27L	TNFSF7	*Bos taurus*	XM_600347	XP_600347
Cf_CD27L	TNFSF7	*Canis lupus familiaris*	XM_542136	XP_542136
Hs_CD27L	TNFSF7	*Homo sapiens*	NM_001252	NP_001243
Mm_CD27L	TNFSF7	*Mus musculus*	NM_011617	NP_035747
Mmu_CD27L	TNFSF7	*Macaca mulatta*	XM_001088935	XP_001088935
Rn_CD27L	TNFSF7	*Rattus norvegicus*	NM_001106878	XP_001059337
Bt_41BBL	TNFSF9	*Bos taurus*	XM_600015	XP_600015
Cf_41BBL	TNFSF9	*Canis lupus familiaris*	XM_533933	XP_533933
Hs_41BBL	TNFSF9	*Homo sapiens*	NM_003811	NP_003802
Mm_41BBL	TNFSF9	*Mus musculus*	NM_009404	NP_033430
Mmu_41BBL	TNFSF9	*Macaca mulatta*	XM_001088828	XP_001088828
Rn_41BBL	TNFSF9	*Rattus norvegicus*	NM_181384	NP_852049
Bt_TRAIL	TNFSF10	*Bos taurus*	XM_583785	XP_583785
Hs_TRAIL	TNFSF10	*Homo sapiens*	NM_003810	NP_003801
Mm_TRAIL	TNFSF10	*Mus musculus*	NM_009425	NP_033451
Mmu_TRAIL	TNFSF10	*Macaca mulatta*	XM_001084768	XP_001084768
Pt_TRAIL	TNFSF10	*Pan troglodytes*	XM_001165714	XP_001165714
Rn_TRAIL	TNFSF10	*Rattus norvegicus*	NM_145681	NP_663714
Bt_RANKL	TNFSF11	*Bos taurus*	XM_591585	XP_591585
Cf_RANKL	TNFSF11	*Canis lupus familiaris*	XM_846672	XP_851765
Hs_RANKL	TNFSF11	*Homo sapiens*	NM_003701	NP_003692
Mm_RANKL	TNFSF11	*Mus musculus*	NM_011613	NP_035743
Mmu_RANKL	TNFSF11	*Macaca mulatta*	XM_001092211	XP_001092211
Pt_RANKL	TNFSF11	*Pan troglodytes*	XM_522750	XP_522750
Rn_RANKL	TNFSF11	*Rattus norvegicus*	NM_057149	NP_476490
Bt_LIGHT	TNFSF14	*Bos taurus*	NM_001101855	NP_001095325
Cf_LIGHT	TNFSF14	*Canis lupus familiaris*	XM_849235	XP_854328
Dr_LIGHT	TNFSF14	*Danio rerio*	XM_001338537	XP_001338573
Hs_LIGHT	TNFSF14	*Homo sapiens*	NM_003807	NP_003798
Mm_LIGHT	TNFSF14	*Mus musculus*	NM_019418	NP_062291
Mmu_LIGHT	TNFSF14	*Macaca mulatta*	XM_001089169	XP_001089169
Pt_LIGHT	TNFSF14	*Pan troglodytes*	Xm_001149848	XP_001149848
Rn_LIGHT	TNFSF14	*Rattus norvegicus*	XM_001059278	XP_001059278
Cf_GITRL	TNFSF18	*Canis lupus familiaris*	XM_848899	XP_853992
Dr_GITRL	TNFSF18	*Danio rerio*	EU099310	ABV22578
Hs_GITRL	TNFSF18	*Homo sapiens*	NM_005092	NP_005083
Mm_GITRL	TNFSF18	*Mus musculus*	NM_183391	NP_899247
Mmu _GITRL	TNFSF18	*Macaca mulatta*	NM_001040191	NP_001035281
Pt_GITRL	TNFSF18	*Pan troglodytes*	XM_001147996	XP_001147996
Rn_GITRL	TNFSF18	*Rattus norvegicus*	XM_344166	XP_344167

or control MOs, all of which resulted in apparently normal embryonic development (Fig. 3). This is consistent with our inability to detect *gitr* message during this period of development. We independently demonstrated that the efficacy of the splice-block *gitrl* MO persisted for the length of the experimental observation (Fig. 3B), and established that it induced mis-splicing of exon 1 to exon 3 resulting in a frame-shift and the introduction of a premature stop codon, such that any resulting protein would completely lack the TNF region required for multimerisation and receptor binding (Fig. 3C).

The majority of *gitrl* morphants showed delayed and abnormal gastrulation, abnormal somitogenesis, abnormal neurogenesis, decreased growth and high mortality. From 70-100% epiboly, morphants had a noticeable developmental lag compared to controls and showed mild perturbations of shape (Fig. 3 E,J). It was also noticeable that the blastoderm margin in *gitrl* morphants did not reach its normal full extent by the end of epiboly (Fig. 3J), and abnormalities were consistently observed by the beginning of segmentation (Fig. 3K). Anterior somites formed, but lacked clear boundaries (Fig. 3 K,L), and although posterior somites had clearer boundaries, they failed to form the characteristic chevron shape observed in control embryos (Figs. 3H, M, magnified in Fig. 3 S,T). The optic primordium appeared late in morphants and remained small and misshapen (Fig. 3 L,M). Morphants remained consistently smaller and had abnormal yolk extensions (Fig. 3M).

We noticed that the *gitrl* morphant embryos had a reduced notochord anlage (data not shown) suggesting possible reduction of cell movements (Kane *et al.*, 1996, Krens *et al.*, 2008). To examine this phenotype more closely, we used the molecular markers *dlx3* (the edge neural plate marker) and *hgg1* (the presumptive hatching gland marker) to compare the *gitrl* morphant phenotypes to control embryos (Krens *et al.*, 2008). The neural plate domain was wider in the *gitrl* morphants, as indicated by the broadened *dlx3* expression domain (Fig. 3 U,V), confirming that

TABLE 2

TNFRSF MEMBERS USED FOR PHYLOGENETIC ANALYSIS

Label in tree (Fig. 1)	Protein	Species	Transcript accession #	Protein accession #
Bt_OX40	TNFRSF4	*Bos Taurus*	NM_001099043	NP_001092513
Cf_OX40	TNFRSF4	*Canis lupus familiaris*	XM_546720	XP_546720
Hs_OX40	TNFRSF4	*Homo sapiens*	NM_003327	NP_003318
Mm_OX40	TNFRSF4	*Mus musculus*	NM_011659	NP_035789
Mmu_OX40	TNFRSF4	*Macaca mulatta*	XM_001090870	XP_001090870
Pt_OX40	TNFRSF4	*Pan troglodytes*	XM_513705	XP_513705
Rn_OX40	TNFRSF4	*Rattus norvegicus*	NM_013049	NP_037181
Bt_CD40	TNFRSF5	*Bos Taurus*	NM_001105611	NP_001099081
Cf_CD40	TNFRSF5	*Canis lupus familiaris*	NM_001002982	NP_001002982
Hs_CD40	TNFRSF5	*Homo sapiens*	NM_001250	NP_001241
Mm_CD40	TNFRSF5	*Mus musculus*	NM_011611	NP_035741
Rn_CD40	TNFRSF5	*Rattus norvegicus*	NM_134360	NP_599187
Ss_CD40	TNFRSF5	*Sus scrofa*	NM_214194	NP_999359
Bt_FAS	TNFRSF6	*Bos Taurus*	NM_174662	NP_777087
Dr_FAS	TNFRSF6	*Danio rerio*	XM_685355	XP_690447
Hs_FAS	TNFRSF6	*Homo sapiens*	NM_000043	NP_000034
Mm_FAS	TNFRSF6	*Mus musculus*	NM_007987	NP_032013
Pt_FAS	TNFRSF6	*Pan troglodytes*	XM_001139138	XP_001139138
Rn_FAS	TNFRSF6	*Rattus norvegicus*	NM_139194	NP_631933
Bt_CD27	TNFRSF7	*Bos Taurus*	NM_001082434	NP_001075903
Cf_CD27	TNFRSF7	*Canis lupus familiaris*	XM_849371	XP_854464
Hs_CD27	TNFRSF7	*Homo sapiens*	NM_001242	NP_001233
Mm_CD27	TNFRSF7	*Mus musculus*	NM_001033126	NP_001028298
Mmu_CD27	TNFRSF7	*Macaca mulatta*	XM_001104258	XP_001104258
Pt_CD27	TNFRSF7	*Pan troglodytes*	XM_508952	XP_508952
Rn_CD27	TNFRSF7	*Rattus norvegicus*	NM_001024335	NP_001019506
Bt_41BB	TNFRSF9	*Bos Taurus*	NM_001035336	NP_001030413
Cf_41BB	TNFRSF9	*Canis lupus familiaris*	XM_845243	XP_850336
Dr_41BB	TNFRSF9	*Danio rerio*	XM_001923079	XP_001923114
Hs_41BB	TNFRSF9	*Homo sapiens*	NM_001561	NP_001552
Mm_41BB	TNFRSF9	*Mus musculus*	NM_001077509	NP_001070977
Mmu_41BB	TNFRSF9	*Macaca mulatta*	XM_001096166	XP_001096166
Pt_41BB	TNFRSF9	*Pan troglodytes*	XM_001157732	XP_001157732
Rn_41BB	TNFRSF9	*Rattus norvegicus*	NM_001025773	NP_001020944
Bt_RANK	TNFRSF11A	*Bos Taurus*	XM_609364	XP_609364
Cf_RANK	TNFRSF11A	*Canis lupus familiaris*	XM_541077	XP_541077
Hs_RANK	TNFRSF11A	*Homo sapiens*	NM_003839	NP_003830
Mm_RANK	TNFRSF11A	*Mus musculus*	NM_009399	NP_033425
Pt_RANK	TNFRSF11A	*Pan troglodytes*	XM_523949	XP_523949
Bt_OPG	TNFRSF11B	*Bos Taurus*	NM_001098056	NP_001091525
Cf_OPG	TNFRSF11B	*Canis lupus familiaris*	XM_539146	XP_539146
Hs_OPG	TNFRSF11B	*Homo sapiens*	NM_002546	NP_002537
Mm_OPG	TNFRSF11B	*Mus musculus*	NM_008764	NP_032790
Mmu_OPG	TNFRSF11B	*Macaca mulatta*	XM_001096915	XP_001096915
Pt_OPG	TNFRSF11B	*Pan troglodytes*	XM_519921	XP_519921
Rn_OPG	TNFRSF11B	*Rattus norvegicus*	NM_012870	NP_037002
Hs_LIGHTR	TNFRSF14	*Homo sapiens*	NM_003820	NP_003811
Rn_LIGHTR	TNFRSF14	*Rattus norvegicus*	NM_001015034	NP_001015034
Mm_LIGHTR	TNFRSF14	*Mus musculus*	NM_178931	NP_849262
Cf_LIGHTR	TNFRSF14	*Canis lupus familiaris*	XM_549666	XP_549666
Mmu_LIGHTR	TNFRSF14	*Macaca mulatta*	NM_001043357	NP_001036822
Bt_GITR	TNFRSF18	*Bos Taurus*	XM_594408	XP_594408
Cf_GITR	TNFRSF18	*Canis lupus familiaris*	XM_843467	XP_848560
Dr_GITR	TNFRSF18	*Danio rerio*	EU099311	NP_001106996
Hs_GITR	TNFRSF18	*Homo sapiens*	NM_004195	NP_004186
Mm_GITR	TNFRSF18	*Mus musculus*	NM_009400	NP_033426
Mmu_GITR	TNFRSF18	*Macaca mulatta*	XM_001090511	XP_001090511
Pt_GITR	TNFRSF18	*Pan troglodytes*	XM_001144377	XP_001144377

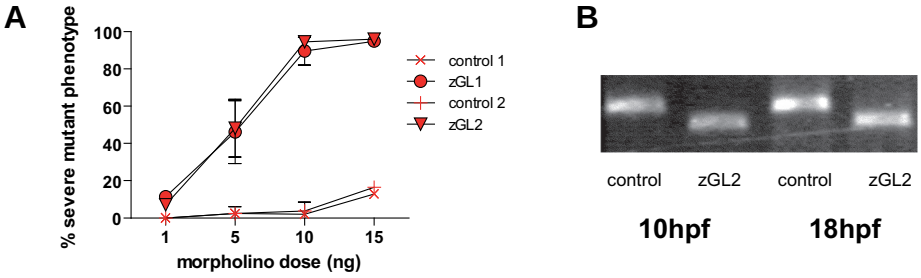

C

Transmembrane

```
control  MSLSAEHCRDTSGDRGGGGGFNGALIHQRTLIRGLIIWVTLLTLGLAASISLHFIPKESPAPSKQQG
zGL2     MSLSAEHCRDTSGDRGGGGGFNGALIHQRTLIRGLIIWVTLLTLGLAASISLHFIPKESPAPSKQQG

control  SETTSNNVYPGKKIDLMTFTPNWENTDVELLQWNTVEERFIKGEGQLTVTQGGAYFLYLQVTLDSRK
zGL2     KTQMLSSCSGIQLKKGSSKERDS-------------------------------------------

control  KENHTITVQTQKQNVILKGYINGSNLSSGFLATGIYLDDDDTFNVTCKPKAKIQNSHIETYMGVIKLG
zGL2     ------------------------------------------------------------------
```

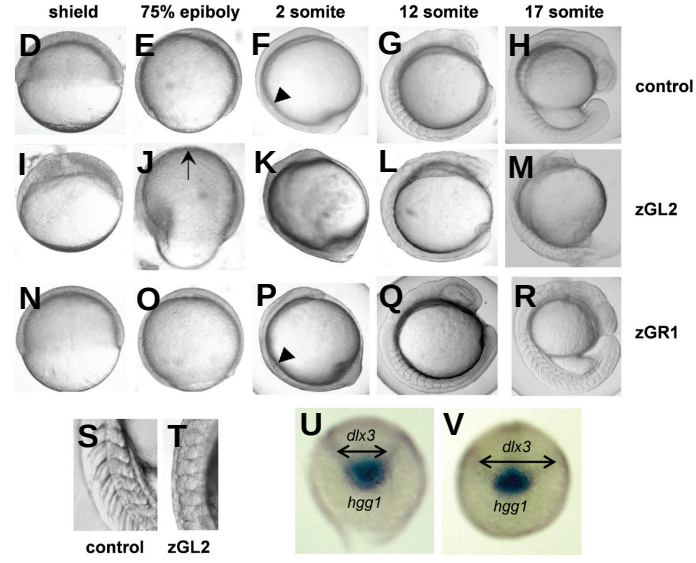

Fig. 3. Morpholino oligonucleotide knock-down of *gitrl* during early development. (A) *Embryos injected with increasing amounts of zGL1 (translation block), zGL2 (splicing block) or control MO were scored at 24 hpf for occurrence of a severe mutant phenotype defined by lack of clear somite boundaries and significant shortening of the embryo. The results are shown graphically as a mean percentage of total embryos injected ± SD of three experiments, with a minimum of 50 embryos injected per MO dose per experiment. Both zGL1 and zGL2 were equivalent in mediating the mutant effect which was not observed with control MOs.* **(B)** *The efficiency and persistence of the splice-blocking MO zGL2 were confirmed using RT-PCR. Following injection of 10 ng of zGL2, but not control MO, a smaller* gitrl *amplification product, diagnostic for the absence of exon 2, was obtained. The effect of zGL2 on splicing remained fully effective to at least 18 hpf.* **(C)** *To confirm the omission of exon 2, transcripts were cloned from zGL2 and control MO injected embryos and a total of 24 control and 48 zGL2 derived clones sequenced. All of the zGL2 derived clones displayed exon 1-3 splicing. This mis-splicing introduced a frameshift mutation such that the TNF family domain region, underlined, would be replaced by an alternative, tuncated C-terminus, indicated in blue. All of the control clones contained the full-length* gitrl *sequence.* **(D-R)** *Embryos injected with control, zGL2 and zGR1 MOs were compared from early gastrula through late segmentation stages. During gastrulation the blastoderm margin was poorly defined at the shield stage* **(I)** *in zGL2 morphants and did not advance to cover the whole of the yolk cell* **(J)**. *Embryos tended to become mildly deformed during epiboly and the dorsal thickening and ventral thinning that is characteristic of late gastrulation was mispositioned in approximately 50 % of the embryos as indicated by the arrow in (J). In contrast both control* **(D,E)** *and zGR1* **(N,O)** *MO-injected embryos remained phenotypically normal during gastrulation. The first somite boundary was clearly delineated in control (arrowhead in* **(F)***) and zGR1 (arrowhead in* **(P)***) but not in zGL2 morphant* **(K)** *embryos. Abnormal somite shape, optic primordium and head shape can be seen in* **(L)**. *By late segmentation, zGL2 MO-injected embryos were significantly shorter with abnormal yolk extensions and abnormally-shaped somites* **(M)**. *A magnified view of the posterior somites clearly shows the normal chevron shape in controls* **(S)** *and the abnormal shape and less-clearly defined boundaries in zGL2 morphants* **(T)**. *(Equivalent phenotypes were also observed using the zGL1 and zGR2, data not shown).* **(U)** *Control or* **(V)** gitrl *morphants were probed at the tail-bud stage (10 hpf) using antisense RNA probes specific for* hgg1 *and* dlx3. *Double-headed arrows indicate the increased width of the* dlx3 *expression domain in* gitrl *morphants relative to control embryos. Data are representative of embryos from at least three independent experiments in which a minimum of thirty embryos per MO per experiment were injected.*

gitrl morphants have reduced cell movement during gastrulation.

Co-injection of synthetic capped *gitrl* mRNA was used to demonstrate the specificity of the MO knockdowns and as little as 100 pg of mRNA was sufficient to prevent the morphant phenotype, while control mRNA had no effect (Fig. 4).

Strain-dependent enhancement of the gitrl *morphant phenotype*

The initial MO knockdown experiments were carried out on embryos from the wild type AB* zebrafish line. When these experiments were repeated using wild type TL embryos, a more extreme form of the phenotype emerged (Fig. 5). In both the translation block and splice-site *gitrl* MO-injected AB* embryos, the blastoderm margin advanced more slowly than in controls and failed to reach its full extent by the end of epiboly (Fig. 5 G-H). In TL embryos, this became more marked as the embryo contracted in on itself (Fig. 5 J-L), eventually pinching off a segment of yolk and dying (Fig. 5L). Sequencing the genomic DNA of ten individual AB* and TL fish embryos from stocks used in our experiments revealed no polymorphisms in the zGL1 target region, suggesting that it is other differences within the genetic background of these two fish lines that ultimately underlie the differential severity of the *gitrl*–MO-induced morphant phenotype.

Linking Gitrl to the Stat3 signalling pathway during early development

Activation of the Stat3 pathway is required for cell movements in zebrafish embryogenesis (Yamashita *et al.*, 2002), raising the possibility that the normal function of Gitrl may include the modulation of Stat3 phosphorylation. We assayed for levels of the

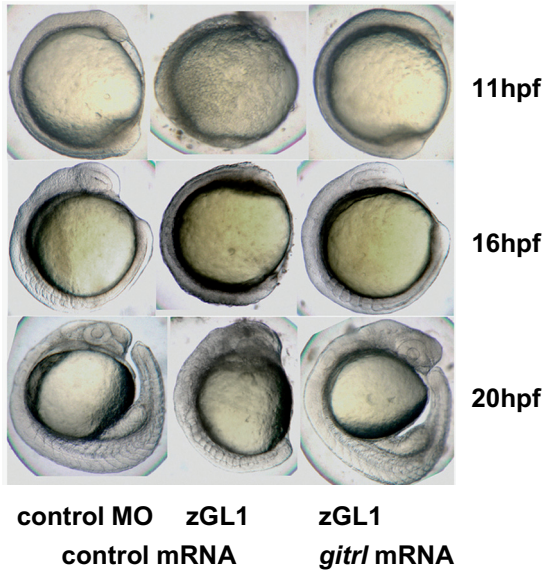

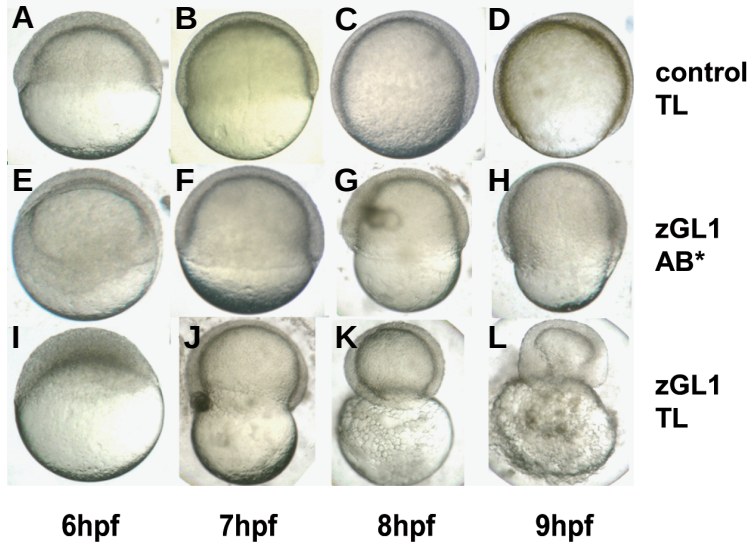

Fig. 4 (Left). Rescue of the MO-induced *gitrl* morphant phenotype by co-injection of synthetic capped *gitrl* mRNA. *Co-injection of synthetic capped mRNA and rescue of a normal phenotype was used to confirm that the MO-induced* gitrl *phenotype was specific and not due to off-target effects. Results with zGL1 (translation block) are shown, although equivalent rescue was also obtained for zGL2 (splice-block). The data are representative of embryos from at least three independent experiments in which a minimum of thirty embryos per MO per experiment were injected.*

Fig. 5 (Right). Strain-dependent penetrance of the MO-induced *gitrl* morphant phenotype. *Embryos of the* **(A-D, I-L)** *TL and* **(E-H)** *AB* strains were injected with 10 ng of either* **(A-D)** *control 1 or* **(E-L)** *zGL1 MO. In zGL1-injected AB* embryos advancement of the blastoderm margin was delayed and incomplete* **(F-H)***, but these embryos successfully completed epiboly and survived through the segmentation period (see Fig. 3). In contrast, zGL1-injected TL embryos could not complete epiboly, and demonstrated a progressive contraction of the embryos around the yolk* **(J-L)**.

activated, phosphorylated form of Stat3 protein by western blot and observed strong phosphorylation of Stat3 during the first 19 hours of development (Fig. 6A). Importantly, levels of phosphorylated Stat3 were decreased at all time points in the *gitrl* morphants. If one function of Gitrl is to modulate Stat3 signalling during embryogenesis, we hypothesised that inhibitors of this pathway might partially phenocopy the *gitrl* knockdown. As observed in *gitrl* morphants, treatment of 2-4 hpf embryos with cucurbitacin I (data not shown) or stattic (Fig. 6 G-K) resulted in delayed and incomplete advancement of the blastoderm margin (Fig. 6G) and indistinct somite boundaries (Fig. 6 H-K). We observed evidence of strain differences in response to Stat3 inhibition, with mortality

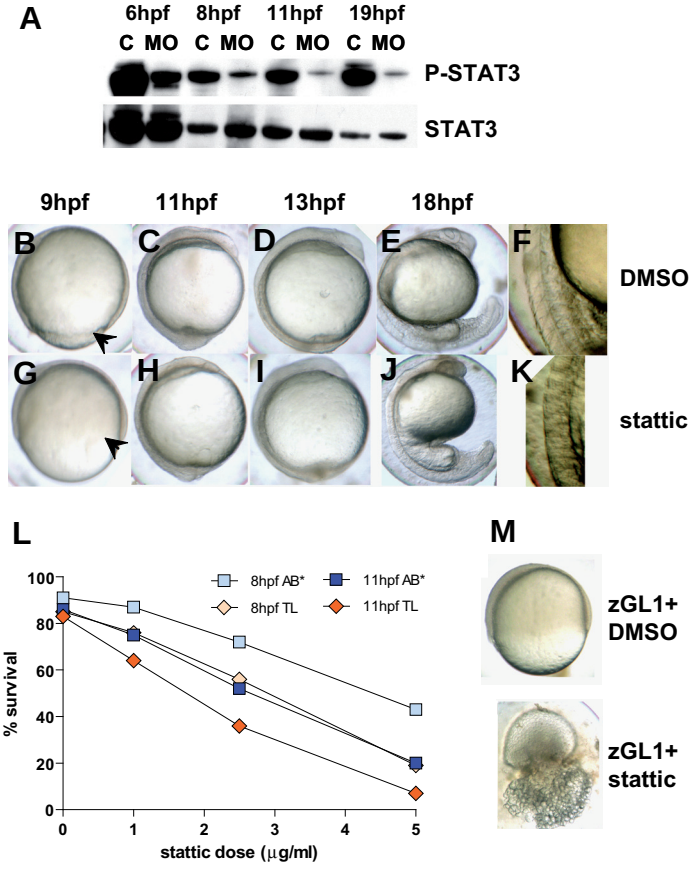

Fig. 6. Identification of Stat3 phosphorylation as a possible mediator of Gitrl effects during embryogenesis. **(A)** *Total protein lysates were generated from embryos injected with 10 ng of control1 (C) or zGL1 (MO) and harvested at 6, 8, 11 and 19 hpf. The lysates were analysed by western blotting using antibodies specific for phosphorylated (P-Stat3) and total (Stat3) Stat3 content. Embryos (AB*) treated with* **(B-F)** *DMSO or* **(G-K)** *5 µM of stattic at 2-4 hpf were compared for phenotypic overlap with the* gitrl *morphant phenotype shown in figure 3. Stattic-treated embryos displayed incomplete blastoderm margin advancement (arrowhead in* **(G)***) compared to controls (arrowhead in* **(B)***), and indistinct somite boundary formation* **(H-K)** *similar to that seen in* gitrl *morphants.* **(L)** *TL embryos were more sensitive than AB* embryos to Stat3 inhibition.* **(M)** *TL embryos treated with a low dose of zGL1 (2.5 ng) were additionally treated with either DMSO or 2 mM of stattic at 2 hpf. Embryos that received low-dose MO plus DMSO were viable, but showed incomplete blastoderm margin advancement at 75 % epiboly, while embryos treated with low-dose zGL1 in addition to treatment with stattic showed a lethal phenotype.*

to increasing concentrations of stattic higher among TL embryos than AB* embryos at both 8 and 11 hpf (Fig. 6L). Additionally, treatment with stattic increased the severity of the morphant phenotype in TL embryos given low doses of *gitrl* MO (Fig. 6M). Although Stat3 is essential for cell movement during gastrulation (Yamashita *et al.*, 2002), subsequent to gastrulation and somitogenesis Stat3 and *gitrl* MO-induced morphants display different phenotypes, suggesting that while Gitrl may act upon Stat3 during early embryogenesis, decreased Stat3 signalling cannot fully account for the effects of *gitrl* knockdown.

Stat3 regulates expression of the zinc transporter Liv1, the activity of which in turn regulates nuclear localisation of the zinc-finger protein Snail (Yamashita *et al.*, 2004), which itself represses transcription of the cell adhesion molecule Cdh1 (Cano *et al.*, 2000). In *gitrl* morphants, we found normal *cdh1* mRNA levels prior to 5 hpf, but observed decreased *liv1* expression and increased *cdh1* expression between 6 and 19 hpf (Fig. 7A). We wondered if the gastrulation-related effects of *gitrl* knockdown were due to increased *cdh1*, and asked if knocking down *cdh1* by MO could at least partially rescue the *gitrl* MO-induced morphant phenotype (Fig. 7 B-I). To our surprise, co-injection of both *gitrl* and *cdh1* MOs led to early arrest, with complete failure to begin gastrulation (Fig. 7 D,H). As *cdh1* expression levels in *gitrl* morphants appeared normal prior to 5 hpf, one possibility is that Gitrl has a Cdh1-dependent function prior to the onset of gastrulation, and only later in development affects the Stat3-Liv1-Cdh1 axis.

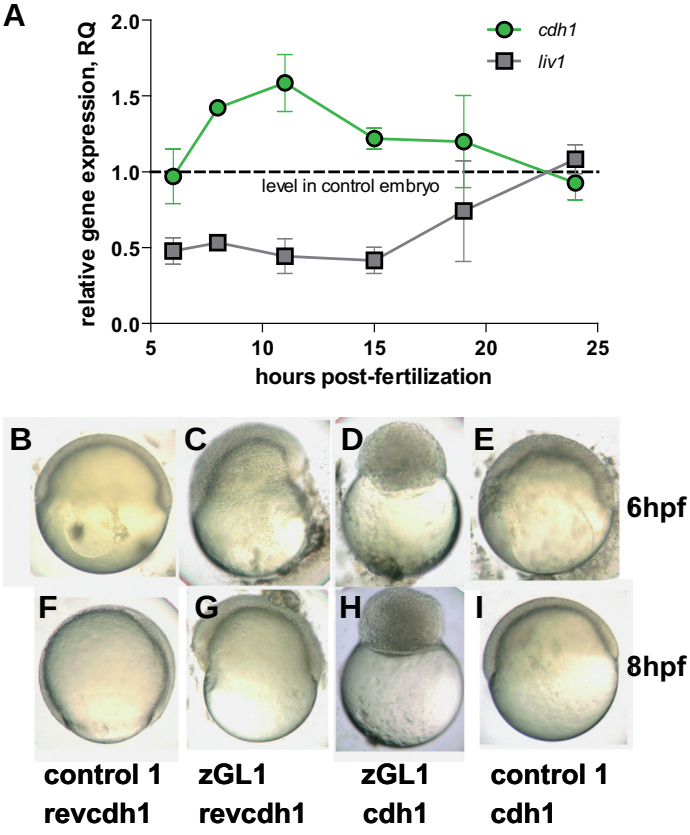

Fig. 7. Gitrl and the Stat3-Liv1-Cdh1 axis. (A) *Transcription of* liv1 *and* cdh1 *were assessed by real-time PCR at various time points during gastrulation and segmentation in embryos injected with 10 ng of either control1 or zGL1. Values were normalised to* ef1α *and levels in zGL1 injected embryos expressed relative to levels detected in control-injected embryos using the ΔΔCt method (ABI Prism 7700 Sequence Detection System, user bulletin no. 2). Mean values ± SD of three independent experiments are shown. Embryos injected with either* **(B,F)** *10 ng of control 1 + 2.5 ng of* cdh1 *MO control (revcdh1),* **(C,G)** *10 ng of zGL1 + 2.5 ng revcdh1,* **(D,H)** *10 ng of zGL1 + 2.5 ng of* cdh1 *MO (cdh1) or (**E,I**) 10 ng of control 1 + 2.5 ng of cdh1 were observed at* **(B-E)** *6 and* **(F-I)** *8 hpf. Embryos treated with control MOs only were indistinguishable from wild-type embryos. Those treated with the zGL1 plus revcdh1 showed the characteristics of* gitrl *morphants previously described, and embryos injected with* cdh1 *MO plus control1 resembled the* avalanche *mutant (Kane* et al.*, 1996). Surprisingly, embryos co-injected with both* gitrl *and* cdh1 *MOs had a novel phenotype characterized by arrest during the blastula period and a complete failure to enter epiboly. The phenotype shown in* **(D)** *and* **(H)** *persisted until the embryos died at approximately 15 hpf.*

Discussion

GITRL and GITR play an important role in the regulation of immune responses in mammals with signalling through GITR increasing resistance to certain tumours and infections, as well as limiting the ability of regulatory cells to suppress the immune response. While *Gitr* knockout mice are viable, and display altered T cell, inflammatory and anti-microbial responses, we found that loss of GITRL was strain-dependently lethal in early embryogenesis in mice (manuscript in preparation). The optical transparency of developing zebrafish offered a unique opportunity to investigate this embryonic lethal effect further, and we consequently sought to identify zebrafish GITRL and GITR homologues.

Putative *gitrl* and *gitr* exons were identified within zebrafish genomic databases by homology and the corresponding full-length transcripts cloned. Assignment of both genes was supported by phylogenetic clustering of the cloned nucleotide coding regions with well-characterised mammalian homologues. While expression of zebrafish *gitr* was detected in adult kidney, spleen, thymus and gut, it was not detected during early development, and embryos developed normally in the presence of *gitr* specific MOs. The *gitr* gene maps to chromosome 6 on the current zebrafish genome build (assembly Zf7). There is no obvious synteny with mouse or human *gitr*, however the lack of impact of *gitr*-targeted MOs and absence of mRNA expression in early embryogenesis are consistent with the viable status of *Gitr* knockout mice, and the documented role of GITR in controlling the mammalian immune response (Agostini *et al.*, 2005, Cuzzocrea *et al.*, 2006, Ronchetti *et al.*, 2002, Shimizu *et al.*, 2002, Tone *et al.*, 2003). MOs targeted against *gitrl* gave rise to a complex developmental phenotype displaying effects on multiple systems. Approximately 15-20% of MOs are known to show off-target effects, which can indeed include somite abnormalities similar to those observed here, however two independent *gitrl* MOs, one blocking translation and the other blocking splicing, both gave rise to the same developmental phenotype and the *gitrl* morphant phenotype was specifically rescued by complementation with synthetic capped *gitrl*, but not control mRNA. Thus the complex morphant phenotype observed here appears to be *gitrl*-specific and, coupled with the multiphasic and localised expression pattern observed in the first 24 hpf, suggests that zebrafish Gitrl has

a role at more than one point in early embryogenesis.

Although none of the reported TNF or TNFR superfamily members knocked out in mice to date have been associated with an embryonic lethal phenotype, family members have been implicated in development, for example, of the secondary lymphoid system (Fu and Chaplin, 1999). RANKL has been shown to regulate osteoclastogenesis, in addition to roles in lymph-node organogenesis and lymphocyte development (Kong *et al.*, 1999), while mutations in EDA have indicated involvement in skin, hair and tooth morphogenesis (Ferguson *et al.*, 1997, Kere *et al.*, 1996). We entered into this investigation seeking insight into the embryonic lethal phenotype that we had encountered in the absence of GITRL in mice. Our data now suggest the possible involvement of an alternative receptor, or else a role for reverse signalling through the ligand (Sun and Fink, 2007). It is not uncommon for TNFSF ligands to bind more than one receptor, however, it has been shown that human and mouse GITRL do not bind to any other currently known mammalian TNFRSF members (Bossen *et al.*, 2006), and so if there is an alternative GITRL receptor involved in murine embryonic development then it has not yet been identified. The phenomenon of reverse signalling has been described for some TNFSF members and was postulated as a mechanism by which soluble GITR could enhance secretion of matrix metalloproteinase 9 (MMP9) from macrophages, although this effect has more recently been shown to be due to blockade of GITR-induced MMP-9 inhibition (Suvas *et al.*, 2005). None of the GITRL sequences have the cytoplasmic casein kinase I motif, -SXXS-, that has been associated with reverse signalling (Sun and Fink, 2007).

We have shown that zebrafish Gitrl influences Stat3 phosphorylation, and raised the possibility that decreased Stat3 phosphorylation in the ligand morphants is responsible for a co-ordinate decrease in *liv1* and increase in *cdh1* expression, leading to increased cell-cell adhesion affecting cell movement (Yamashita *et al.*, 2004). This could be sufficient to account for the slow and incomplete nature of gastrulation in the morphants. Nevertheless, our experiments with Stat3 inhibition, as well as published work on *stat3* MO effects (Yamashita *et al.*, 2002), show that decreased Stat3 signalling does not fully account for the observed *gitrl* morphant phenotype. This suggests that there are other mechanisms of development affected, and the kinetics of *gitrl* expression, with multiple expression peaks, would imply independent effects at different time-points.

We observed strain dependent differences in the affects of *gitrl* knockdown in zebrafish. There were no nucleotide polymorphisms in the relevant MO target sequence, eliminating this as an explanation of the difference. There was evidence of differing sensitivity to Stat3 inhibition, raising the possibility that constitutive differences in Stat3 signalling exist between the two test strains. That the effects of Gitrl loss can be enhanced on specific genetic backgrounds offers the possibility of future genetic and small molecule screens to identify modulators of this pathway in early development.

Previous mining of teleost genomes described fourteen distinct TNFSF member genes, but failed to identify clear orthologs of four genes encoding members involved in mammalian T cell activation and homeostasis, namely OX40L, CD27L, CD30L and GITRL (Glenney and Wiens, 2007). In humans and mice, the GITRL gene is located on chromosome 1, flanked by genes encoding FASL and OX40L. Genes encoding LIGHT, CD27L and 4-1BBL form a separate TNFSF cluster on human chromosome 19/mouse chromosome 17. Here, we assigned zebrafish *gitrl* based on homology and protein alignment data, which was supported by phylogenetic cluster analysis of nucleotide coding regions (Fig. 1). We note that this sequence has been placed on the current zebrafish genome build (assembly Zf7) downstream of *light*, in a position consistent with mammalian *4-1BBL.* Interestingly, the gene annotated as zebrafish *light* did not group with mammalian *LIGHT* homologues in the nucleotide based phylogenetic analysis shown in Fig. 1C. It did move to the LIGHT grouping when the phylogeny was repeated using protein data (data not shown). The zebrafish Gitrl also moved to group with mammalian 4-1BBL homologues in this analysis; although by pairwise alignment the zebrafish Gitrl shared lower identity with human and mouse 4-1BBL, than the GITRL homologues (13 *versus* 18 %), and the reverse signalling casein kinase I motif conserved in mammalian 4-1BBL homologues was absent from zebrafish Gitrl (Sun and Fink, 2007), both features failing to support this alternate gene assignment. Furthermore, while embryonic defects have not been reported in mice lacking 4-1BBL (DeBenedette *et al.*, 1999), both the absence of GITRL in mice and knockdown of the proposed *gitrl* in zebrafish generated a strain dependant embryonic lethal phenotype.

In general terms the zebrafish immune system has proved remarkably similar to that of mammals, and is being developed to model human disease (Meeker and Trede, 2008). Here we have identified and cloned TNF/TNFRSF members related by homology and phylogenetic analysis to mammalian GITRL and GITR. We have demonstrated a multiphasic pattern of *gitrl* expression in the first 24 hpf, and that knockdown of this expression gives rise to a complex phenotype to reveal a critical requirement for Gitrl in early embryogenesis, at the very least involved in gastrulation. These effects are mediated prior to the expression of Gitr, its only currently known receptor in mammals. Our studies implicating Gitrl in the control of Stat3 signalling during early zebrafish development provide an initial platform for future studies to determine if Gitrl can also regulate Stat3 signalling in mouse development. In conclusion our data has established that Gitrl, which came to prominence because of its role in regulation of the mammalian immune system, also has a previously unappreciated role in vertebrate embryonic development mediated independently of Gitr.

Materials and Methods

Fish stocks

Adult zebrafish of the AB* and TL strains were maintained on a 14hr/10hr light/dark cycle at 28.5°C. Embryos were staged according to (Kimmel *et al.*, 1995).

Human and mouse GITRL and GITR transcripts were used to query the zebrafish genome using blastn. Putative coding sequences were assembled from the genomic data and full-length coding sequences PCR-amplified and cloned to pGEM-T easy (Promega) using primers:

gitrl

5'-TCACTACTGCATCATGTCTCTGT-3' and

5'-TGACTGAGATTTAGCCAAGCTTGATGACA-3', and

gitr

ACGCATTGGTAATGCACCACAGTG-3' and

5'-AGGAAAGCTGTGGTCACAGCAGT-3'.

Multiple clones were sequenced. Sequence alignments were performed using Jalview 2.4 (Waterhouse *et al.*, 2009).

Phylogenetic analysis

Closely related superfamily members were identified using human and mouse GITRL and GITR and the newly identified zebrafish sequences to query the nr database by tblastn. For the ligand, TNFSF5, 7, 10 and 11 were included on the basis of sequence homology, TNFSF4, 6, 9 and 14 by genomic proximity and ectodysplasin and EIGER were also included. For the receptor, TNFRSF4, 5, 9, 11 and 14 were included on the basis of tblastn and TNFRSF6 and 7 to complement the ligand analysis. Species homologues were identified, but only those with synteny information supporting their assignment were included (at least one flanking gene identified). Multiple sequence FASTA files of ligand and receptor nucleotide coding and protein sequences were compiled and analysed using the 'one-click' phylogeny application, at http://www.phylogeny.fr/ (without GBlock refinement) (Dereeper *et al.*, 2008).

RNA isolation and real-time PCR

RNA was extracted from adult tissues or whole embryos using the SV Total RNA Isolation System (Promega) and reverse transcribed using the Stratascript First Strand Synthesis System (Stratagene). Real-time PCR was performed as previously described (Nolan *et al.*, 2004) using the following primers and probes:
zgitrl primers
5'-CTAATGACATTCACGCCAAACTG-3' and
5'-CAGCTGTCCCTCTCCTTTGATG-3' and
probe
5'FAM-TTCCACTGCAGGAGCTCAACATCTGTGT-3';
zgitr primers
5'-GCTGTAAAGCCTGTCCTGCAT-3' and
5'-GAAGGGCATTTCTCACACAGACT-3' and
probe
5'FAM-CCTATATCGGCATGTTCACAAGACAGGACA-3';
*zef1*α primers
5'-CCACGTCGACTCCGGAAA-3' and
5'-CGATTCCACCGCATTTGTAGA-3' and
probe 5'VIC-TCCACCACCACCGGCCATCTG-3';
zliv1 primers
5'- GCTGAACGCGCTTACTTTCG -3' and
5'- CAGCAGTGCCAGTGACATCAC -3' and
probe
5'FAM- CGTGGACTCCCGGTTGCCAATATG -3';
zcdh1 primers
5'- CTGCTATTGCTTGCTCTTCTTCTG -3' and
5'- CATCATAATAGTAGATGTTGTCCCGTACA -3' and
probe
5'FAM- TCCTGCGGAGGAAAAGCAACTCCAA -3'.

For each of three biological replicates, embryos were pooled from timed mating of 8-10 pairs of fish and collected at the indicated time-points over a contiguous period.

In situ *hybridisation*

Whole-mount *in situ* hybridisation was carried out as described by (Thisse and Thisse, 2008). Antisense RNA probes were transcribed from linearised templates using T3, T7, or SP6 RNA polymerases (Promega) in the presence of digoxigenin (DIG)–labelled nucleotides (Roche). DIG was detected using anti-DIG-alkaline phosphatase Fab and BM-Purple (Roche). For the *gitrl* candidate the probe was synthesised from the full-length coding sequence. The probe constructs for *dlx3* and *hgg1* were a kind gift of Jeroen den Hertog (Utrecht, The Netherlands).

Morpholino oligonucleotides (MOs)

Antisense MOs were designed by and obtained from GeneTools (Philomath, OR)
zGL1 5'-TTCGGCAGACAGAGACATGATGCAG-3' (translation block);
zGL2 5'-TTAAATGGTGACTTACAGTTTGGCG-3' (splice block exon1-exon2);
control 1 5'-GACGTAGTACAGAGACAGACGGCTT-3' (reverse of zGL1);
control 2 5'-GCGGTTTGACATTCAGTGGTAAATT-3' (reverse of zGL2);
zGR1 5'-TGTTCATTCTGTCACTGTGGTGCAT-3' (translation block); and
zGR2 5'-GATATAGGATACTCGCCTGTACAAT-3' (splice block exon1-exon2).
The antisense splicing-blocking MO for e-cadherin, *cdh1*, was that described by (Shimizu *et al.*, 2005):
5 2-AAAGTCTTACCTGAAAAAGAAAAAC-3 2. The reverse sequence was used as control.

Stock solutions, 10 μg/μL of each MO, were prepared in Danieau buffer, and 1 to 15 ng of stock solution, or specified dilutions, injected into 1-4 cell-stage embryos using a Picospritzer II microinjector (Parker Instrumentation). The efficiency of the splice-blocking zGL2 MO was monitored by RT-PCR using the full-length *gitrl* primers described above. Efficiency of the zGR2 splice-blocking MO could not be determined because *gitr* could not be amplified from either control or experimental groups in the first two days of development.

Capped mRNA synthesis

Capped, polyadenylated mRNA for zebrafish *gitrl* and for mouse *Tnf* (control RNA) was *in vitro* transcribed from pGEM-T easy plasmids using SP6 or T7 mMessage mMachine kits (Ambion, Austin, TX) and injected into embryos at the one-cell stage. One replicate of the rescue experiment was done blinded to eliminate the possibility of observer bias.

Western blotting

Protein lysates were separated on denaturing SDS-PAGE gels, transferred to a PDVF membrane and probed using anti-zebrafish phospho-Stat3 (MBL International), or anti-Stat3 (Santa Cruz) primary, and peroxidase-conjugated secondary antibodies. Antibody binding was detected using ECL solutions (Pierce).

Treatment of embryos with inhibitors

Stock solutions of cucurbitacin I (Calbiochem) or stattic (Calbiochem) dissolved in DMSO were added at the stated concentrations to embryos in 6-well plates. Control embryos were treated with DMSO alone at the same concentrations.

Acknowledgements

We thank Jeroen den Hertog (Hubrecht Institute, Utrecht, Netherlands) for in situ *hybridization plasmids, Masahiko Hibi (RIKEN, Japan) for experimental advice and plasmids, Nick Temperley (MRC Human Genetics Unit & The University of Edinburgh, UK) and Fernando Martinez (SWDSOP, Oxford, UK) for support regarding bioinformatics, Elizabeth Robertson (SWDSOP, Oxford, UK) for advice on the manuscript, and Roger Patient and his laboratory (WIMM, Oxford, UK) for experimental discussion. This work was supported by an MRC Programme Grant, HW, and an MRC Career Development Award, EEP.*

References

AGOSTINI, M., CENCI, E., PERICOLINI, E., NOCENTINI, G., BISTONI, G., VECCHIARELLI, A. and RICCARDI, C. (2005). The glucocorticoid-induced tumor necrosis factor receptor-related gene modulates the response to Candida albicans infection. *Infect Immun* 73: 7502-7508.

BOSSEN, C., INGOLD, K., TARDIVEL, A., BODMER, J.L., GAIDE, O., HERTIG, S., AMBROSE, C., TSCHOPP, J. and SCHNEIDER, P. (2006). Interactions of tumor necrosis factor (TNF) and TNF receptor family members in the mouse and human. *J Biol Chem* 281: 13964-13971.

CANO, A., PEREZ-MORENO, M.A., RODRIGO, I., LOCASCIO, A., BLANCO, M.J., DEL BARRIO, M.G., PORTILLO, F. and NIETO, M.A. (2000). The transcription factor snail controls epithelial-mesenchymal transitions by repressing E-cadherin

expression. *Nat Cell Biol* 2: 76-83.

CUZZOCREA, S., NOCENTINI, G., DI PAOLA, R., AGOSTINI, M., MAZZON, E., RONCHETTI, S., CRISAFULLI, C., ESPOSITO, E., CAPUTI, A.P. and RICCARDI, C. (2006). Proinflammatory role of glucocorticoid-induced TNF receptor-related gene in acute lung inflammation. *J Immunol* 177: 631-641.

DEBENEDETTE, M.A., WEN, T., BACHMANN, M.F., OHASHI, P.S., BARBER, B.H., STOCKING, K.L., PESCHON, J.J. and WATTS, T.H. (1999). Analysis of 4-1BB ligand (4-1BBL)-deficient mice and of mice lacking both 4-1BBL and CD28 reveals a role for 4-1BBL in skin allograft rejection and in the cytotoxic T cell response to influenza virus. *J Immunol* 163: 4833-4841.

DEREEPER, A., GUIGNON, V., BLANC, G., AUDIC, S., BUFFET, S., CHEVENET, F., DUFAYARD, J.F., GUINDON, S., LEFORT, V., LESCOT, M. *et al.* (2008). Phylogeny.fr: robust phylogenetic analysis for the non-specialist. *Nucleic Acids Res* 36: W465-469.

FERGUSON, B.M., BROCKDORFF, N., FORMSTONE, E., NGYUEN, T., KRONMILLER, J.E. and ZONANA, J. (1997). Cloning of Tabby, the murine homolog of the human EDA gene: evidence for a membrane-associated protein with a short collagenous domain. *Hum Mol Genet* 6: 1589-1594.

FRATTINI, A., VEZZONI, P., VILLA, A. and SOBACCHI, C. (2007). The Dissection of Human Autosomal Recessive Osteopetrosis Identifies an Osteoclast-Poor Form due to RANKL Deficiency. *Cell Cycle* 6: 3027-3033.

FU, Y.X. and CHAPLIN, D.D. (1999). Development and maturation of secondary lymphoid tissues. *Annu Rev Immunol* 17: 399-433.

GLENNEY, G.W. and WIENS, G.D. (2007). Early diversification of the TNF superfamily in teleosts: genomic characterization and expression analysis. *J Immunol* 178: 7955-7973.

KANE, D.A., HAMMERSCHMIDT, M., MULLINS, M.C., MAISCHEIN, H.M., BRAND, M., VAN EEDEN, F.J., FURUTANI-SEIKI, M., GRANATO, M., HAFFTER, P., HEISENBERG, C.P. *et al.* (1996). The zebrafish epiboly mutants. *Development* 123: 47-55.

KERE, J., SRIVASTAVA, A.K., MONTONEN, O., ZONANA, J., THOMAS, N., FERGUSON, B., MUNOZ, F., MORGAN, D., CLARKE, A., BAYBAYAN, P. *et al.* (1996). X-linked anhidrotic (hypohidrotic) ectodermal dysplasia is caused by mutation in a novel transmembrane protein. *Nat Genet* 13: 409-416.

KIMMEL, C.B., BALLARD, W.W., KIMMEL, S.R., ULLMANN, B. and SCHILLING, T.F. (1995). Stages of embryonic development of the zebrafish. *Dev Dyn* 203: 253-310.

KONG, Y.Y., YOSHIDA, H., SAROSI, I., TAN, H.L., TIMMS, E., CAPPARELLI, C., MORONY, S., OLIVEIRA-DOS-SANTOS, A.J., VAN, G., ITIE, A. *et al.* (1999). OPGL is a key regulator of osteoclastogenesis, lymphocyte development and lymph-node organogenesis. *Nature* 397: 315-323.

KRENS, S.F., HE, S., LAMERS, G.E., MEIJER, A.H., BAKKERS, J., SCHMIDT, T., SPAINK, H.P. and SNAAR-JAGALSKA, B.E. (2008). Distinct functions for ERK1 and ERK2 in cell migration processes during zebrafish gastrulation. *Dev Biol* 319: 370-383.

MEEKER, N.D. and TREDE, N.S. (2008). Immunology and zebrafish: spawning new models of human disease. *Dev Comp Immunol* 32: 745-757.

MORENO, E., YAN, M. and BASLER, K. (2002). Evolution of TNF signaling mechanisms: JNK-dependent apoptosis triggered by Eiger, the *Drosophila* homolog of the TNF superfamily. *Curr Biol* 12: 1263-1268.

NOLAN, K.F., STRONG, V., SOLER, D., FAIRCHILD, P.J., COBBOLD, S.P., CROXTON, R., GONZALO, J.A., RUBIO, A., WELLS, M. and WALDMANN, H. (2004). IL-10-conditioned dendritic cells, decommissioned for recruitment of adaptive immunity, elicit innate inflammatory gene products in response to danger signals. *J Immunol* 172: 2201-2209.

RONCHETTI, S., NOCENTINI, G., RICCARDI, C. and PANDOLFI, P.P. (2002). Role of GITR in activation response of T lymphocytes. *Blood* 100: 350-352.

SHIMIZU, J., YAMAZAKI, S., TAKAHASHI, T., ISHIDA, Y. and SAKAGUCHI, S. (2002). Stimulation of CD25(+)CD4(+) regulatory T cells through GITR breaks immunological self-tolerance. *Nat Immunol* 3: 135-142.

SHIMIZU, T., YABE, T., MURAOKA, O., YONEMURA, S., ARAMAKI, S., HATTA, K., BAE, Y.K., NOJIMA, H. and HIBI, M. (2005). E-cadherin is required for gastrulation cell movements in zebrafish. *Mech Dev* 122: 747-763.

SUN, M. and FINK, P.J. (2007). A new class of reverse signaling costimulators belongs to the TNF family. *J Immunol* 179: 4307-4312.

SUVAS, S., KIM, B., SARANGI, P.P., TONE, M., WALDMANN, H. and ROUSE, B.T. (2005). *In vivo* kinetics of GITR and GITR ligand expression and their functional significance in regulating viral immunopathology. *J Virol* 79: 11935-11942.

THISSE, C. and THISSE, B. (2008). High-resolution *in situ* hybridization to whole-mount zebrafish embryos. *Nat Protoc* 3: 59-69.

TONE, M., TONE, Y., ADAMS, E., YATES, S.F., FREWIN, M.R., COBBOLD, S.P. and WALDMANN, H. (2003). Mouse glucocorticoid-induced tumor necrosis factor receptor ligand is costimulatory for T cells. *Proc Natl Acad Sci U S A* 100: 15059-15064.

WATERHOUSE, A.M., PROCTER, J.B., MARTIN, D.M., CLAMP, M. and BARTON, G.J. (2009). Jalview Version 2—a multiple sequence alignment editor and analysis workbench. *Bioinformatics* 25: 1189-1191.

YAMASHITA, S., MIYAGI, C., CARMANY-RAMPEY, A., SHIMIZU, T., FUJII, R., SCHIER, A.F. and HIRANO, T. (2002). Stat3 Controls Cell Movements during Zebrafish Gastrulation. *Dev Cell* 2: 363-375.

YAMASHITA, S., MIYAGI, C., FUKADA, T., KAGARA, N., CHE, Y.S. and HIRANO, T. (2004). Zinc transporter LIVI controls epithelial-mesenchymal transition in zebrafish gastrula organizer. *Nature* 429: 298-302.

YE, H., PARK, Y.C., KREISHMAN, M., KIEFF, E. and WU, H. (1999). The structural basis for the recognition of diverse receptor sequences by TRAF2. *Mol Cell* 4: 321-330.

ZELENIKA, D., ADAMS, E., HUMM, S., GRACA, L., THOMPSON, S., COBBOLD, S.P. and WALDMANN, H. (2002). Regulatory T cells overexpress a subset of Th2 gene transcripts. *J Immunol* 168: 1069-1079.

Further Related Reading, published previously in the *Int. J. Dev. Biol.*

See our recent Special Issue ***Epigenetics & Development*** edited by Saadi Khochbin and Stefan Nonchev at:
http://www.ijdb.ehu.es/web/contents.php?vol=53&issue=2-3

Expression of zinc transporter family genes in Dictyostelium
Nobuya Sunaga, Meri Monna, Nao Shimada, Mai Tsukamoto and Takefumi Kawata
Int. J. Dev. Biol. (2008) 52: 377-381

A change in response to Bmp signalling precedes ectodermal fate Choice
Chris T. Dee, Abigail Gibson, Andrea Rengifo, Shun-Kuo Sun, Roger K. Patient and Paul J. Scotting
Int. J. Dev. Biol. (2007) 51: 79 - 84

Evidence that the rat osteopetrotic mutation toothless (tl) is not in the TNFSF11 (TRANCE, RANKL, ODF, OPGL) gene
P R Odgren, N Kim, L van Wesenbeeck, C MacKay, A Mason-Savas, F F Safadi, S N Popoff, C Lengner, W van-Hul, Y Choi and S C Marks
Int. J. Dev. Biol. (2001) 45: 853-859

Tumor necrosis factor-alpha inhibits epithelial differentiation and morphogenesis in the mouse metanephric kidney *in vitro*
C M Cale, N J Klein, G Morgan and A S Woolf
Int. J. Dev. Biol. (1998) 42: 663-674

Distribution of TNF alpha-like proteins correlates with some regions of programmed cell death in the chick embryo
M A Wride, P H Lapchak and E J Sanders
Int. J. Dev. Biol. (1994) 38: 673-682

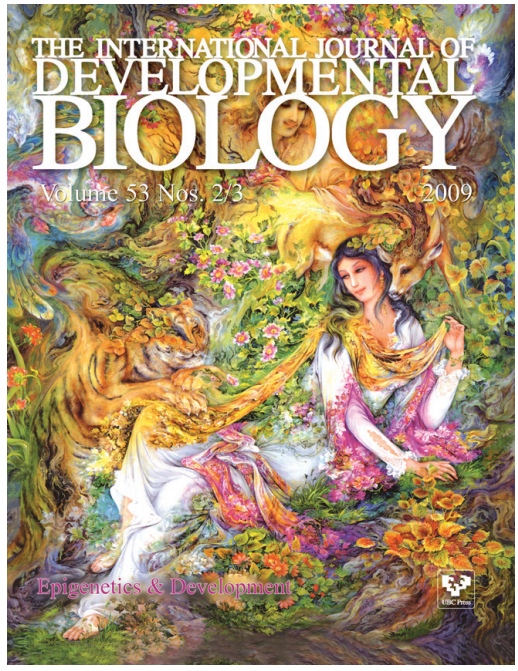

5 yr ISI Impact Factor (2008) = 3.271

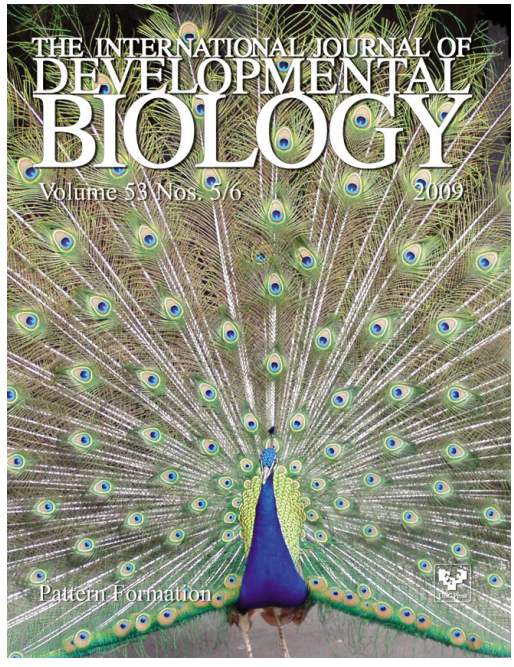

For all the latest on *Pattern Formation* research,
see our latest Special Issue
edited by C.-M. Chuong and M.K. Richardson.

http://www.ijdb.ehu.es/web/contents.php?vol=53&issue=5-6